Chapter 1
Intelligent Digital Twin Assembly Leveraging Bayesian Classification

Shishir Sharma, Nicholas Daly, Stephen Jay Wright, Laura Redmond, Christopher S. McMahan, John R Wagner, and Matthew P. Castanier

Abstract Digital twins can be used for system performance optimization, health monitoring, predictive maintenance, and investigating system anomalies. A ground vehicle digital twin may be assembled using representations of the subsystem models (tires, suspension system, powertrain, etc.) of different fidelity. The objective of this study is to demonstrate the application of Bayesian Classification within a novel tool for selecting subsystem models to construct suitable digital twins. This tool consists of two phases: first, each subsystem model is calibrated to a set of experimentally collected field or laboratory data (or against the highest fidelity model if test data is not available); second, Bayesian classification is used to select a suitable digital twin based on the likelihood of observing the experimental data from that model. If the probability of observing the data from a digital twin assembled from lower fidelity subsystem models is similar to the probability of observing the data from a digital twin composed of higher fidelity subsystem models, then using the lower fidelity option has several significant advantages, including computational time and engineering cost. The proposed tool can assess many possible mixtures of fidelities among subsystems and thus select only the high-fidelity representations where they are truly needed. A demonstration of the Bayesian Classification method is provided using a wheeled ground vehicle dynamics model

Shishir Sharma
Graduate Research Assistant, Department of Civil Engineering, Clemson University, S Palmetto Blvd, Clemson, SC 29634
e-mail: shishis@clemson.edu

Nicholas Daly
Graduate Research Assistant, Clemson University, Fluor Daniel Building, 216 South Palmetto Boulevard, Clemson, SC 29634-0921
e-mail: ndaly@g.clemson.edu

Stephen Jay Wright
Graduate Research Assistant, Clemson University, Lowry Hall: 306 S. Palmetto Blvd, Clemson, SC 29634
e-mail: swrigh7@g.clemson.edu

Laura Redmond
Associate Professor, School of Civil and Environmental Engineering and Earth Sciences, and School of Mechanical and Automotive Engineering, Clemson University, 116 Lowry Hall, Clemson, SC, 29634
e-mail: lmredmo@clemson.edu

Christopher S. McMahan
Professor, School of Mathematical and Statistical Sciences,
Clemson University, O-102 Martin Hall, 220 Parkway Drive, Clemson, SC 29634-0975
e-mail: mcmaha2@clemson.edu

John R Wagner
Professor of Mechanical Engineering, PLM Center Director, College of Engineering, Computing and Applied Sciences,
Clemson University, 212 Fluor Daniel Engineering Innovation Building, 216 South Palmetto Boulevard, Clemson, SC 29634-0921
e-mail: jwagner@clemson.edu

Matthew P. Castanier
Research Mechanical Engineer, US Army DEVCOM Ground Vehicle Systems Center,
6501 E. 11 Mile Rd., MS 157, Warren, MI 48397-5000
e-mail: matthew.p.castanier.civ@army.mil

DISTRIBUTION STATEMENT A. Approved for public release; distribution is unlimited. OPSEC10040

Kristin B. Zimmerman, PhD (eds.), *Model Validation and Uncertainty Quantification, 2026, Vol. 3*, Conference Proceedings of the Society for Experimental Mechanics Series, https://doi.org/10.1007/97887-438-1442-9_1

created in Matlab/Simulink. Simulated field data was generated using the highest fidelity model with added white noise. The numerical results show that the innovative classification tool can identify the best combination of tire and suspension subsystem models within a vehicle dynamics model to represent the simulated field data. Future work will include expanding the demonstration to include more digital twin subsystem models and a demonstration with physical data.

Keywords Digital twin · Model selection · Bayesian classification · Mixture modeling · Uncertainty quantification

Introduction

A Digital Twin is a virtual representation of an actual physical asset in operation from the microatomic level to the macro-geometric level that can be used to evaluate the current condition of the asset and predict future behavior, refine control, or optimize operation [3],[13]. It can be developed and used throughout the product life cycle, from design to manufacturing, through deployment operations [19] and for system upgrade evaluations. Digital Twins can effectively reduce costs by enabling virtual testing, integrating physical test outcomes, and facilitating timely, data-driven decisions by providing comprehensive insights into individual components and the asset as a whole [20].

A complex system, such as a ground vehicle, usually has multiple Digital Twins compiled into a single universal Twin [25],[21]. A ground vehicle consists of multiple subsystems like the tires, suspension system, chassis, powertrain, etc. The digital twin to represent a ground vehicle may be assembled using different fidelity representations of such subsystem models. Often a developer's ambition to build a Digital Twin that is identical to the physical system, leads to the creation of an overly complex Digital Twin [26]. However, the fidelity of the subsystem models impacts the computational cost of the Digital Twin. An efficient Digital Twin must balance the fidelity of predictions with the computational demands (time, power and complexity) [2][21].

The selection of an appropriate Digital Twin model has often been conducted through decision-based algorithms selecting the best Digital Twin according to use cases. Such approaches can determine the overall class of model that match the intended service or performance requirements, while not directly considering the appropriateness of the underlying physics or system architecture to adequately capture the output of interest. For example, [14] formulates a decision model for quantification of the suitability of DT applications and targeted selection of data-driven DT applications based on value-effort analysis. Similarly, [1] focuses on prioritizing DT applications based on stakeholders' needs, technical feasibility, business needs, and risk factors.

Physics-based Digital Twin selection methodologies have also been put forth that aim at selecting Digital Twin models based on their ability to replicate the actual physical system behavior. Such methods are often data-driven, developed to match the Digital Twin output to some experimental data from the physical system. Efforts have been made toward the creation and selection of the optimal set of data-based reduced-order component models to comprise a digital twin using optimal decision trees, an interpretable machine learning method [8]. The key differences between this work and that proposed in [8] is that the decision tree does not provide statistical insight into its decision, which would allow a user to select the next best model if the marginal cost in computation time for the increased accuracy of the optimal model was deemed too high. Other notable contributions in this area include Digital Twin selection via dynamic Bayesian networks [7] and reinforcement learning [17]. Unlike, [7] which primarily focuses on updating unknown parameters throughout the lifetime of an asset to account for physical degradation, our approach seeks to identify and calibrate different digital twin assemblies and more aptly accounts for uncertainty propagation throughout the selection process by explicitly accounting for the uncertainty associated with the calibration of each assembly. Further, all evaluations of the digital twin in the proposed approach can be parallelized thereby reducing the total time required to make the selection. In contrast, the technique in [17] must assess a posited assembly at each iteration of their approach; these serial computations would render their proposal intractable for computationally intensive assemblies. Further, given the use of approximate Bayesian computation techniques, the compute time is highly dependent on the number of unknown parameters and their ranges.

We propose a novel mixture-based Bayesian machine learning framework for intelligent selection of Digital Twin assembly by identifying and selecting the appropriate combination of the subsystem models with varying fidelities. While Bayesian methods have been implemented in the Digital Twin domain for model updating [23] or calibrating model parameters [6], the proposed Bayesian Assembly Tool integrates Bayesian model calibration and Bayesian classification to systematically assess Digital Twin models comprised of different combinations of different fidelity subsystem models and select the DT with the most appropriate mixture of subsystem model fidelities while also providing statistical insight to the decision. By embedding engineering models of varying fidelities as components in a mixture model and deploying a reduction mechanism that promotes lower-fidelity model, this framework delivers data-driven, uncertainty-aware, and computationally efficient digital twin assemblies, thereby enhancing parsimony.

The proposed method has five major steps. The first step is to acquire laboratory test data for calibration. The second step involves creating Digital Twin assemblies with combinations of different fidelity subsystem models and calibrating to the lab- oratory test data. The calibration process essentially creates a set of representative output data from each digital twin assembly that is not affected by the improper selection of the uncertain input parameters. Griddy Gibbs calibration methodology [6] has been implemented in this demonstration, which produces posterior distributions of the uncertain model parameters. In the third step, a set of field test data is obtained for classification. This data can be the same as the laboratory test data used for cali- bration or a new one under different known parameter settings. Next, synthetic field data are generated from the Digital Twin Assemblies for the unknown parameters sampled from the posterior distributions obtained from the Griddy Gibbs calibration. The synthetic field data from each assembly is fitted to a multivariate normal distribution with a unique mean and covariance structure. The final step is Bayesian classification, where the probability of observing the field test data given the mean and co- variance of each assembly is evaluated. The model with the highest probability is the best-fitting model selected by the Bayesian Assembly Tool. In addition, the Assembly tool can be used to analyze if more than one combination of the subsystem models fits the observed data based on the probability of observing the data, allowing the users to select the Digital Twin assembly that is least computationally demanding.

Methodology

The workflow of the Bayesian Assembly Tool for Digital Twin selection involves five basic steps, and is schematically shown in Figure 1.

1. *Obtain Laboratory Test Data for Calibration*: Laboratory test data $\boldsymbol{Y} = (\boldsymbol{Y}_1, \boldsymbol{Y}_2, ..., \boldsymbol{Y}_n)$ are obtained from experiments in the physical vehicle or generated from a high-fidelity Digital Twin simulation with added measurement error under known parameters $\boldsymbol{X} = (\boldsymbol{X}_1, \boldsymbol{X}_2, ..., \boldsymbol{X}_n)$. The laboratory test data $\boldsymbol{Y}$ under the known parameters $\boldsymbol{X}$ is denoted by $\boldsymbol{D}$.
2. *Griddy Gibbs Model Calibration*: A suite of Digital Twin assemblies $\boldsymbol{M}_1, \boldsymbol{M}_2, ...\boldsymbol{M}_m$ with different fidelity subsystem models is created, and each of them is calibrated to the laboratory test data $\boldsymbol{Y}$. The Griddy Gibbs calibration method

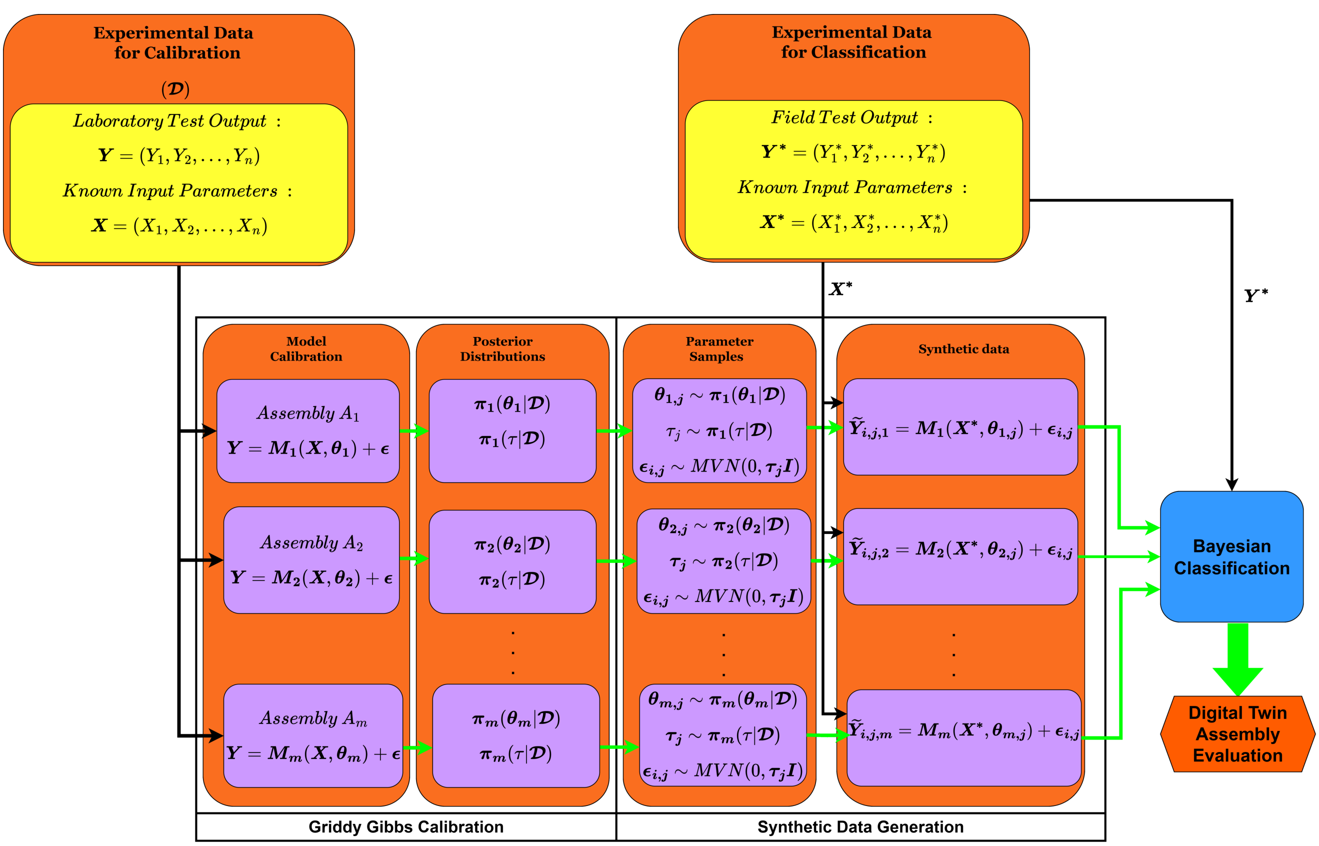

Fig. 1 Bayesian Assembly Tool working flowchart

is used, which produces the posterior distributions $\pi_m(\boldsymbol{\theta}_m|\boldsymbol{D})$ of the uncertain parameters $\boldsymbol{\theta}_m$ and the posterior distributions $\pi_m(\tau_m|\boldsymbol{D})$ of the precision parameter τ_m governing the error distribution from each assembly *m*.

3. *Obtain Field Test Data for Classification*: A set of field test data, $\boldsymbol{Y}^* = (\boldsymbol{Y}^*_1, \boldsymbol{Y}^*_2, ..., \boldsymbol{Y}^*_n)$, is obtained, which may be the same used for the calibration or a new set of data under different known parameter settings $\boldsymbol{X}^* = (\boldsymbol{X}^*_1, \boldsymbol{X}^*_2, ..., \boldsymbol{X}^*_n)$.
4. *Synthetic Field Data Generation from Digital Twin Assemblies*: The uncertain parameters $\boldsymbol{\theta}_{m,j}$ for each Digital Twin Assembly *m* are sampled from their posterior distributions $\pi_m(\boldsymbol{\theta}_m|\boldsymbol{D})$. Then, the Digital Twin Assemblies are evaluated at these parameters $\boldsymbol{\theta}_{m,j}$ under the known parameters $\boldsymbol{X}^*$ to obtain the model output $\boldsymbol{M}_m(\boldsymbol{X}^*, \boldsymbol{\theta}_{m,j})$. The precision parameter $\tau_{m,j}$ is sampled from the posterior distribution $\pi_m(\tau_m|\boldsymbol{D})$, and a Gaussian noise $\boldsymbol{\epsilon}_{m,i,j}$ is sampled from a multivariate normal distribution with $\mathbf{0}$ mean and covariance $\tau^{-1}_{m,j}\,\mathbf{I}$. This noise is added to $\boldsymbol{M}_m(\boldsymbol{X}^*, \boldsymbol{\theta}_{m,j})$ to obtain large sets of synthetic data $\tilde{\boldsymbol{Y}}_{m,i,j}$ from each assembly. Then, a multivariate normal distribution is fitted to the synthetic data, and the corresponding mean vector and covariance matrix are estimated for each of the Digital Twin assemblies.
5. *Model Selection by Bayesian Classification*: The final step is to evaluate the likelihood of obtaining the data $\boldsymbol{Y}^*$ given the mean and covariance structure of each assembly. Based on the relative probability of each assembly and the computational cost associated with the assembly (given different fidelity levels), the optimal Digital Twin assembly can be selected.

Each step of the methodology is described in detail in the subsequent sections.

Obtain Laboratory Test Data for Calibration

A set of experimental laboratory data $\boldsymbol{Y}$ is acquired from the physical vehicle system under known input parameters $\boldsymbol{X}$ (true parameters). This data is used to calibrate the Digital Twin assemblies with various possible combinations of subsystem models of different levels of fidelity. An example of such data could be the time history of normal force on the tire when the vehicle passes over a speed bump. The data can be acquired from laboratory tests of vehicle systems or a controlled field test. However, if such a test is not feasible, simulated laboratory test data can be generated from the highest-fidelity Digital Twin Assembly, and the output can be used to calibrate the other Digital Twin Assemblies under consideration.

Time domain data should be processed to obtain lower resolution data (such as local maxima/minima, data at significant time points, integrated parameters, or frequency-domain responses) to avoid artificially reducing the uncertainty in the posterior distributions given by the Griddy Gibbs calibration.[6]

Griddy Gibbs Model Calibration

The next step is calibrating the Digital Twin assemblies $\boldsymbol{M}_1, \boldsymbol{M}_2, ..., \boldsymbol{M}_m$ of varying fidelity, with the laboratory test data $\boldsymbol{Y}$. There are numerous deterministic and statistical model calibration methods that could be used for this purpose; e.g., see [24].[18],[9]. We have implemented the Bayesian Griddy Gibbs model calibration method developed in [6], except for a slight modification in the optimization process used to identify the feasible region. In particular, in the optimization process used herein, the sum of squared error between laboratory test data $\boldsymbol{Y}$ and the Digital Twin assembly output $\boldsymbol{M}_m(\boldsymbol{X}, \boldsymbol{\theta}_m)$ for unknown parameter settings $\boldsymbol{\theta}_m$ and known parameter settings $\boldsymbol{X}$ is taken as the objective function. By minimizing this objective function, via a non-linear optimization algorithm, we identify an optimal solution $\boldsymbol{\theta}_{mo}$. The normal likelihood of observing the laboratory test data given the model output at the optimal solution as the mean and the maximum likelihood estimate of the covariance as the covariance is evaluated. This likelihood corresponds to the maximum likelihood. Next, to evaluate the feasible region around $\boldsymbol{\theta}_{mo}$, each dimension of $\boldsymbol{\theta}_{mo}$ is iteratively varied by a certain fixed step, keeping the other dimensions fixed at the optimal solution, and the likelihood is calculated at each step. When the likelihood drops to 1% of the maximum likelihood, the algorithm is stopped, and the same process is repeated for the other dimensions of $\boldsymbol{\theta}_{mo}$. In this way, the upper and lower boundaries for $\boldsymbol{\theta}_m$ are computed.

Obtain Field Test Data for Classification

For the final classification of the Digital Twin Assemblies, another data set is required. This data set would preferably come from a field test, but if these data are not available, the classification could be conducted based on the laboratory test data, or simulated field test data can be generated from the highest-fidelity Digital Twin Assembly. Unlike the laboratory test data, the field test data used for classification do not need to be down-sampled or summarized.

Synthetic Field Data Generation from Digital Twin Assemblies

The next step after calibration is to generate synthetic field data from each of the calibrated assemblies. The uncertain parameters $\boldsymbol{\theta}_{m,j}$ are sampled from their respective posterior distributions $\pi_m(\boldsymbol{\theta}_m|\boldsymbol{D})$ obtained from calibration of assembly $\boldsymbol{M}_m$. The number of parameter samples should be sufficient to represent the posterior distributions, which may be less than the number of Griddy Gibbs samples forming the posterior distributions. Digital Twin simulations are run for those parameters under the same known parameter settings $\boldsymbol{X}^*$ as in the field test data to obtain the model output $\boldsymbol{M}_m(\boldsymbol{X}^*, \boldsymbol{\theta}_{m,j})$. The precision parameters $\tau_{m,j}$ are sampled from their posterior distributions $\pi_m(\tau_m|\boldsymbol{D})$, and the Gaussian noise $\boldsymbol{\epsilon}_{m,ij}$ is sampled from a multivariate normal distribution with $\mathbf{0}$ mean and covariance $\tau\,{}^{1}_{m,i,j}\,\mathbf{I}$. This noise is added to the simulation output from the assemblies to obtain the simulated field data $\boldsymbol{Y}^*$ from each assembly, i.e., the synthetic field data is given by:

$$\widetilde{\mathbf{Y}}^*_{m,i,j} = \boldsymbol{M}_m\left(\boldsymbol{X}^*_i, \boldsymbol{\theta}_{m,j}\right) + \boldsymbol{\epsilon}_{m,i,j} \tag{1}$$

A multivariate normal distribution is then fitted to these data, and estimates of the mean vector and covariance matrix are obtained for each of the assemblies. These multivariate normal distributions are used during Bayesian classification for model selection.

Model Selection by Bayesian Classification

The final step is the selection of the appropriate Digital Twin assembly using the Bayesian classification method. This involves evaluating the probability of observing the field test data given the aforementioned multivariate normal distributions of each assembly. This measure provides the relative likelihood of observing the field test data ($\boldsymbol{Y}^*$) under each of the potential assem- blies; i.e., which assembly best aligns with the field test data. The assembly corresponding to the highest likelihood is identified as the best representation for the field data by the Bayesian Assembly Tool.

However, the Digital Twin assembly with the highest probability is not necessarily the best choice overall. In selecting the optimal Digital Twin, the fidelity of different subsystem models should also be considered, along with how frequently the assembly is chosen by the Bayesian Assembly Tool. If a relatively lower-fidelity assembly yields a comparable likelihood of being selected to that of a higher-fidelity one, the lower-fidelity version may be a more efficient option, given the lower computational costs and demands associated with the lower-fidelity model.

Demonstration Problem: Vehicle Dynamics Model in MATLAB Simulink

A Digital Twin model of a wheeled vehicle was created for this demonstration in MATLAB Simulink. Four Digital Twin assemblies were used, consisting of combinations of two tire models and two suspension models, while rest of the subsystems were identical.

Tire Models

The first tire model used was the Fiala tire. The model is available in the Simulink library as “Fiala Wheel 2DOF” block. The Fiala tire model considers the tire acts as a beam on an elastic foundation. It assumes that the contact patch is rectangular and pressure is uniform across it. It neglects the effects of the tire’s camber angle. The model calculates the normal force using equation (2), where the notation mirrors the Matlab documentation; see [5] for further discussion.

$$F_{ztire} = \rho_z k - b\dot{z} \tag{2}$$

The second tire model used was the PAC2002 tire which is relatively more complex than the Fiala model. The “Combined Slip Wheel 2DOF” block available in the Simulink library is used to model the Pac2002 tire [4]. In the PAC2002 model, the vertical tire response is modeled as a spring and a damper in parallel. The contact patch is found assuming the tire acts as a rigid disc. The model calculates the normal force using equation(3).

$$F_z = \left\{1 + q_{V2}\left|\Omega\right|\frac{R_o}{V_o} - \left(q_{Fcx}\frac{F_x}{F_{zo}}\right)^2 - \left(q_{Fcy}\frac{F_y}{F_{zo}}\right)^2\right\}.\left\{\left(q_{Fz1} + q_{Fz3}\gamma^2\right)\frac{\rho_z}{R_o} + q_{Fz2}\frac{\rho_z^2}{R_o^2}\right\}.\left(1 + p_{pFz1}dp_i\right).F_{zo} \tag{3}$$

See Table 3 in Appendix for descriptions of the variables used in equation (3) and [16],[22] for a more discussion.

Suspension Models

The two suspension models were used in the Digital Twin assemblies: MacPherson suspension and solid axle suspension.

The MacPherson suspension model used in the Digital Twin uses a linear spring and damper to model the vertical dynamic ef- fects of the suspension system. Using the relative positions and velocities of the vehicle and wheel carrier, the block calculates the vertical suspension forces on the wheel and vehicle. The block uses a linear equation that relates vertical damping and com- pliance to the suspension height, suspension height rate of change, and absolute value of the steering angles. The MacPherson

suspension is available in the Simulink library as "Independent Suspension - MacPherson". The block implements equation (4) to calculate the suspension force, where the notation mirrors the Matlab documentation; see [11] for a further discussion.

$$F_{wz_{a,t}} = F_{z0_a} + k_{z_a}\left(z_{v_{a,t}} - z_{w_{a,t}} + m_{h\mathrm{steer}_a}\left|\delta_{\mathrm{steer}_{a,t}}\right|\right) + c\left(\dot{z}_{v_{a,t}} - \dot{z}_{w_{a,t}}\right) + F_{zhstop_{a,t}} + F_{zaswy_{a,t}} \tag{4}$$

See Table 4 in Appendix for descriptions of the variables used in equation (4).

Solid axle suspension block used in the Digital Twin models the suspension compliance, damping, and geometric effects as functions of the wheel positions and velocities, with axle-specific compliance and damping parameters. Using wheel position and velocity, the block calculates the vertical wheel position and suspension forces on the vehicle and wheel. The "Solid axle Suspension - Coil Spring" block is used to model the solid axle suspension in Simulink. The block implements equation (5), where the notation mirrors Matlab documentation; see [12] for further discussion.

$$F_{wz_{a,t}} = -F_{wa_{z0}} + k_{wa_z}\left(z_{w_{a,t}} - z_{s_{a,t}}\right) - c_{wa_z}\left(\dot{z}_{w_{a,t}} - \dot{z}_{s_{a,t}}\right) \tag{5}$$

See Table 5 in Appendix for descriptions of the variables used in equation (5).

Implementation of the Bayesian Assembly Tool

Simulated Laboratory Data Generation

To validate the Bayesian assembly tool, four different Digital Twin assemblies were created by combining the two tire and two suspension systems:

- M_1: Pac2002 tire and MacPherson suspension (high-fidelity assembly)
- M_2: Pac2002 tire and Solid axle suspension
- M_3: Fiala tire and MacPherson suspension
- M_4: Fiala tire and Solid axle suspension

The simulated laboratory data was generated from the Digital Twin assembly M_1. The input parameters (true parameters) are shown in Table 1

Table 1 True parameter setting for simulated experimental data generation

Parameter	True value
Tire Stiffness ($\theta(1)$)	180000 N/m
Tire Damping ($\theta(2)$)	3000 Ns/m
Suspension Stiffness ($\theta(3)$)	30000 N/m
Suspension Damping ($\theta(4)$)	2500 Ns/m

The simulated laboratory data was generated under the scenario where the Digital Twin accelerated along a straight path from 0 to 20 mph in the first five seconds and then continued forward with a constant velocity. The road profile used for the simulation was smooth from 0 to 6 seconds. At the sixth second, the front wheel of the vehicle encountered a speed bump 200 mm high and 100 mm long. The road profile was flat for the remainder of the simulation. The road profile used for the simulation is shown in Figure 2, and the reference velocity profile is shown in Figure 3. The model output considered for calibration was the normal force on the left front wheel hub. White noise representing the measurement error was added to the Digital Twin simulation output. The noise was estimated by assuming the measurement would be taken with a $20kN$ force transducer assuming a measurement error of 2%, we took the 3σ error to be $400N$.

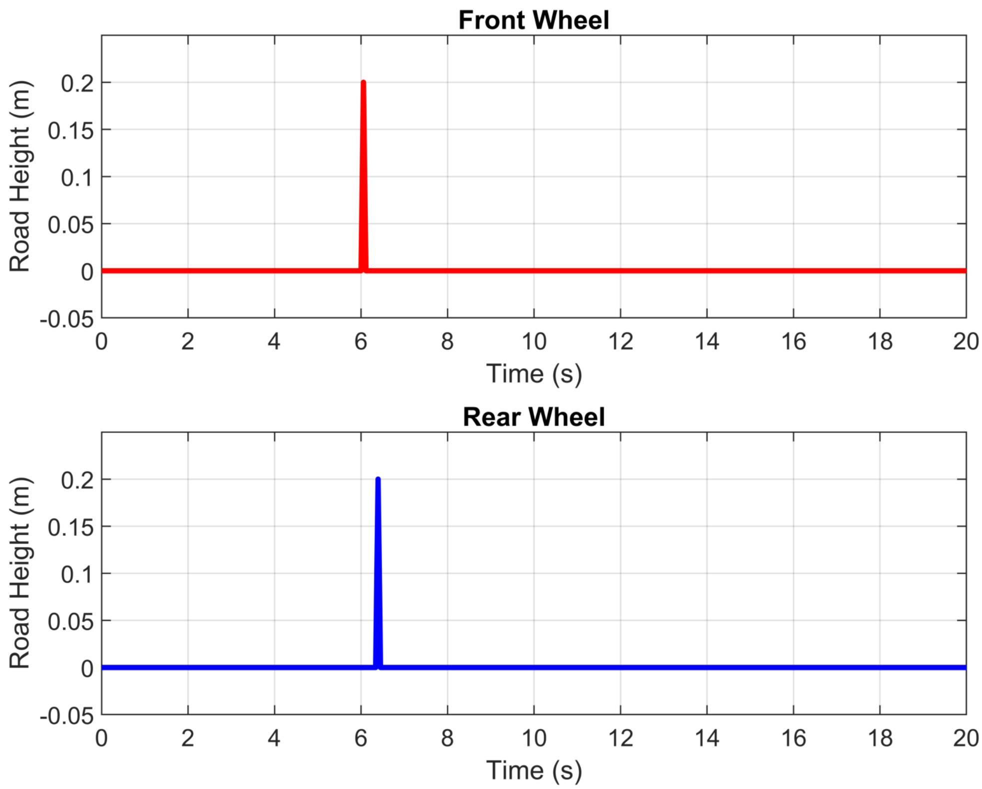

Fig. 2 Road profile for the front and rear wheel (y-axis is road elevation in meters) used in the simulation

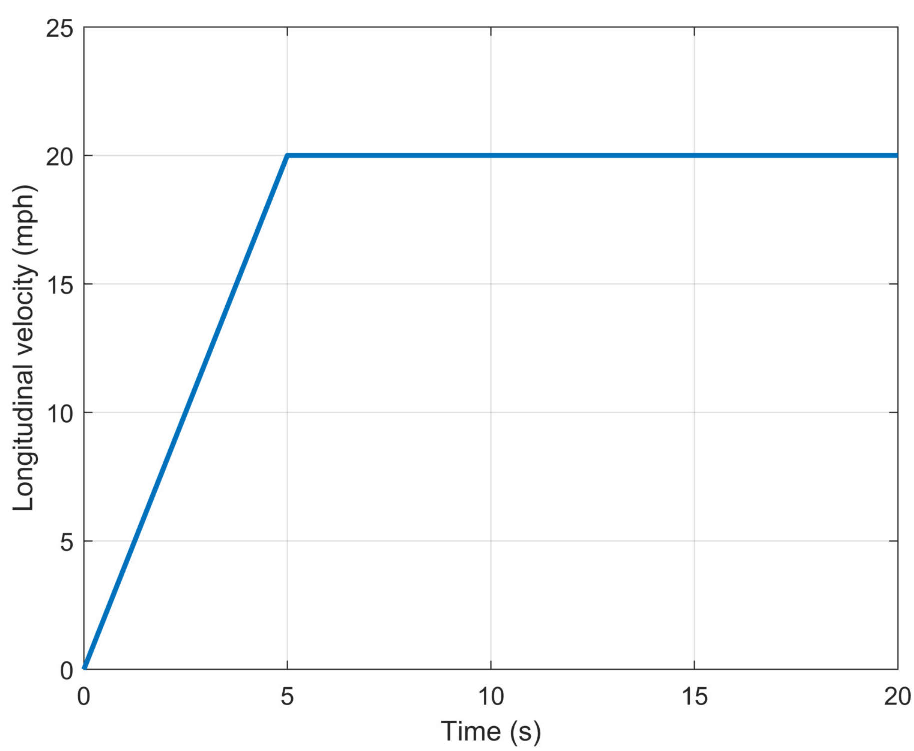

Fig. 3 Longitudinal velocity reference (y-axis is the velocity in mph)

This Gaussian noise was sampled ten times from a normal distribution with 0 mean and 18000N variance and added to the normal force output of the assembly M_1 under the aforementioned true parameters and simulation settings to obtain the ten sets of high-resolution simulated laboratory data, as shown in Figure 4.

The normal force at the wheel hub of the front left tire was originally sampled every 0.001 seconds. Calibrating the Digital Twin assemblies to such high-resolution data would produce a narrow posterior distribution due to an artificial reduction in the uncertainty in the uncertain parameter estimation. To avoid this, the full-time history data was condensed to include only the response at a few significant time points near where local maxima and minima typically occur in the models. Those timesteps were 6.422, 6.558, 6.689, 6.973, and 7.291 seconds. This was the actual simulated laboratory data used for calibration, which is shown in Figure 5.

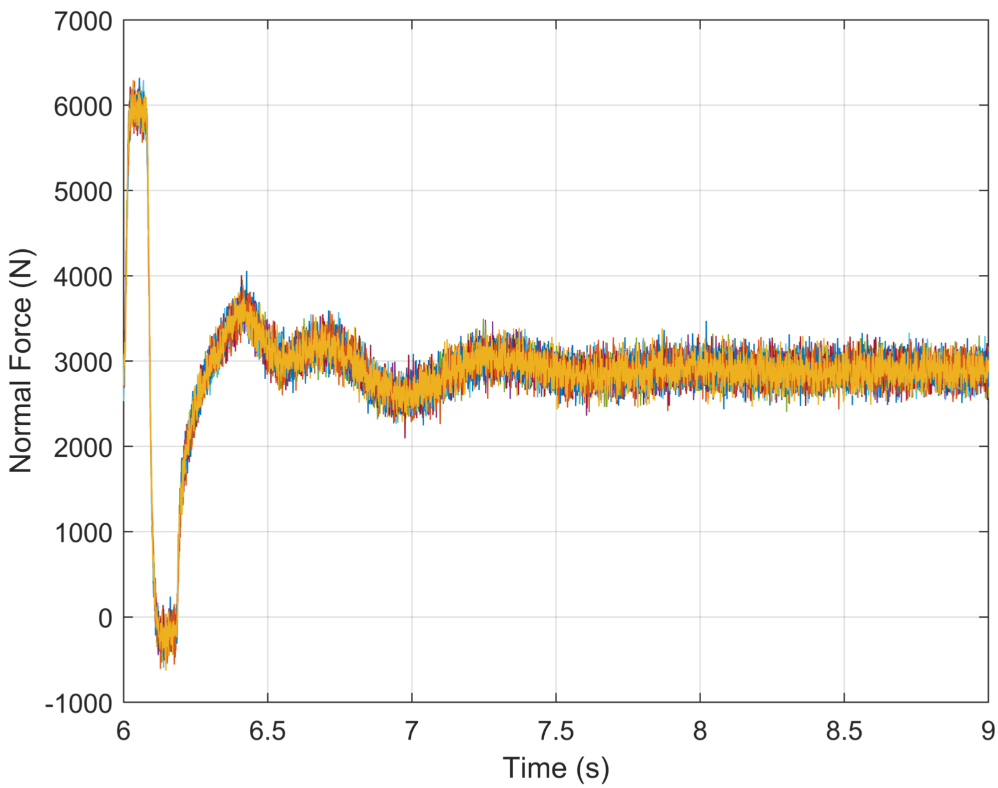

Fig. 4 Simulated experimental data (full time history)

Griddy Gibbs Model Calibration

The four Digital Twin assemblies were calibrated to the condensed simulated laboratory data. First, for each assembly, the full time history of the normal force from the left front wheel hub in the model was down-sampled to only the response at the five time points of the reduced simulated laboratory data. A non-linear optimization algorithm, 'fmincon' [10] in MATLAB, was used to determine the feasible region for the Griddy Gibbs model calibration. The sum of squared error between the simulated experimental data Y and the Digital Twin output $f(\theta, X)$ was the objective function minimized. The constraints for the optimization were the upper and lower boundaries of the four parameters given in Table 2.

After identifying an optimal solution at which to begin defining the feasible region, the upper and lower limits of the feasible region were determined for each parameter, one at a time, keeping the other three parameters at their optimal solution. The boundary of the feasible region was determined by finding the parameter value where the likelihood of observing the output drops to 1% of the maximum likelihood (at the optimal solution). Once the boundaries for all four parameters were set, a grid of 2000 set of parameters was created using Latin Hypercube Sampling and the Digital Twin assembly was evaluated for those parameters. Then, the Griddy Gibbs calibration was run, where 50000 Griddy Gibbs samples of the four uncertain parameters and the precision parameter were taken, 15000 samples were burnt, and the remaining samples formed

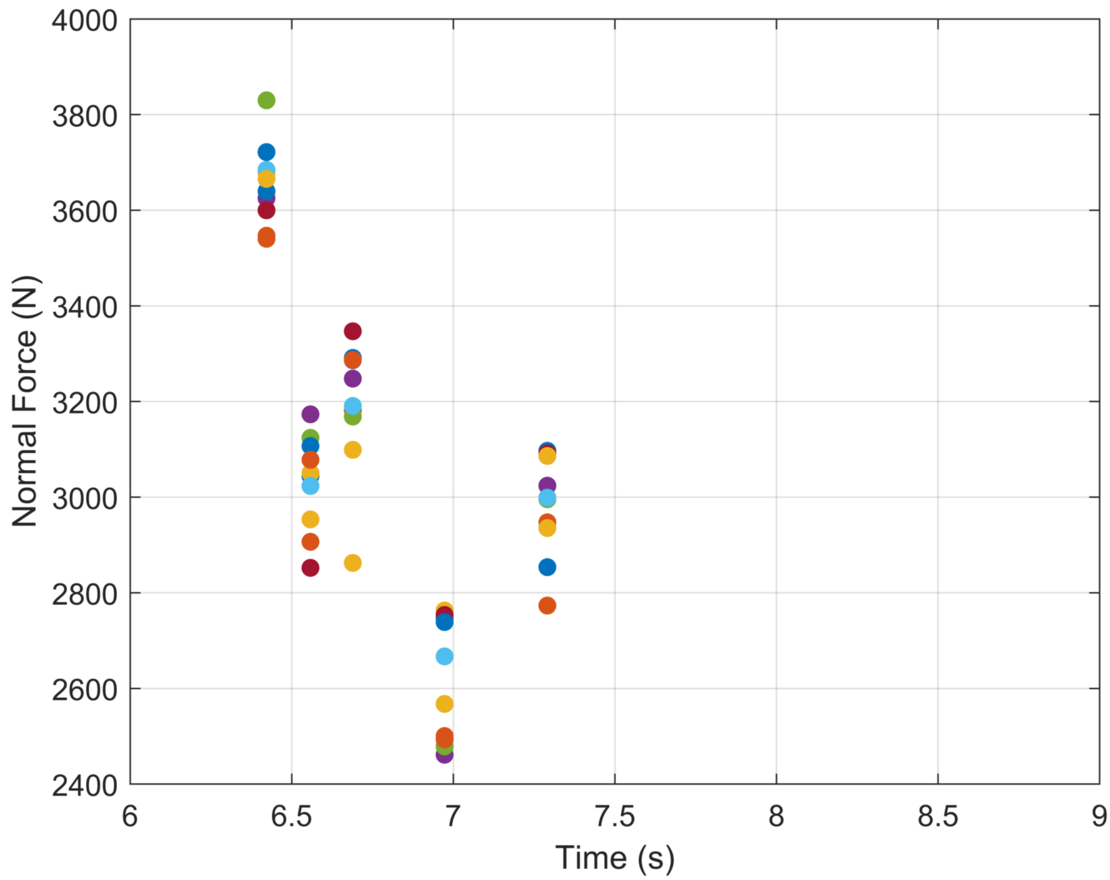

Fig. 5 Simulated laboratory data

Table 2 Calibration Parameters and Ranges for Different Digital Twin Assemblies

Digital Twin Assembly	Calibrating Parameters	Range
Assembly 1 (MacPherson suspension and Pac2002 tire, high-fidelity)	Pac2002 Tire stiffness ($\theta_1(1)$)	120000 to 800000 N/m
	Pac2002 Tire damping ($\theta_1(2)$)	500 to 7000 N·s/m
	Suspension stiffness ($\theta_1(3)$)	10000 to 180000 N/m
	Suspension damping ($\theta_1(4)$)	500 to 30000 N·s/m
Assembly 2 (MacPherson suspension and Fiala tire)	Fiala Tire stiffness parameter ($\theta_2(1)$)	400 to 8000 N/m
	Fiala Tire damping parameter ($\theta_2(2)$)	3000 to 180000 N·s/m
	Suspension stiffness ($\theta_2(3)$)	10000 to 180000 N/m
	Suspension damping ($\theta_2(4)$)	500 to 30000 N·s/m
Assembly 3 (Solid axle suspension and Pac2002 tire)	Pac2002 Tire stiffness ($\theta_3(1)$)	120000 to 800000 N/m
	Pac2002 Tire damping ($\theta_3(2)$)	500 to 7000 N·s/m
	Suspension stiffness ($\theta_3(3)$)	10000 to 180000 N/m
	Suspension damping ($\theta_3(4)$)	500 to 30000 N·s/m
Assembly 4 (Solid axle suspension and Fiala tire)	Fiala Tire stiffness parameter ($\theta_4(1)$)	400 to 8000 N/m
	Fiala Tire damping parameter ($\theta_4(2)$)	3000 to 180000 N·s/m
	Suspension stiffness ($\theta_4(3)$)	10000 to 180000 N/m
	Suspension damping ($\theta_4(4)$)	500 to 30000 N·s/m

the parameters' posterior distributions. This whole process of optimization, boundary evaluation and the Griddy Gibbs calibration was repeated for all four assemblies. The posterior distributions of the four uncertain parameters and the precision parameter of assembly M_1 are shown in Figure 6.

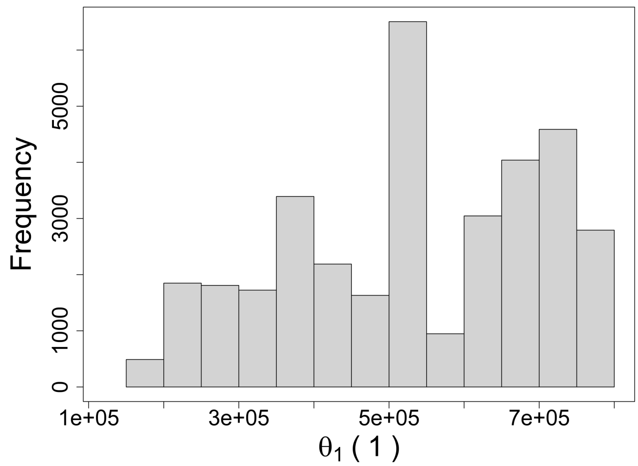

(a) Posterior distribution for $\theta_1(1)$

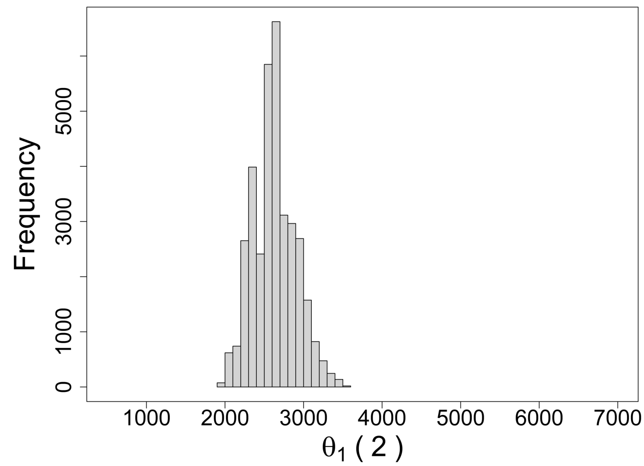

(b) Posterior distribution for $\theta_1(2)$

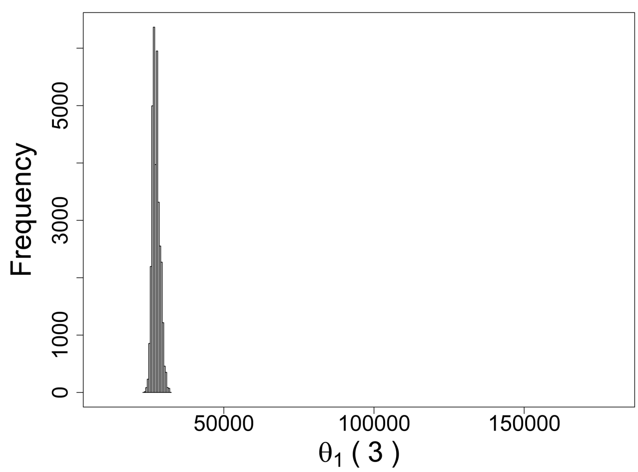

(c) Posterior distribution for $\theta_1(3)$

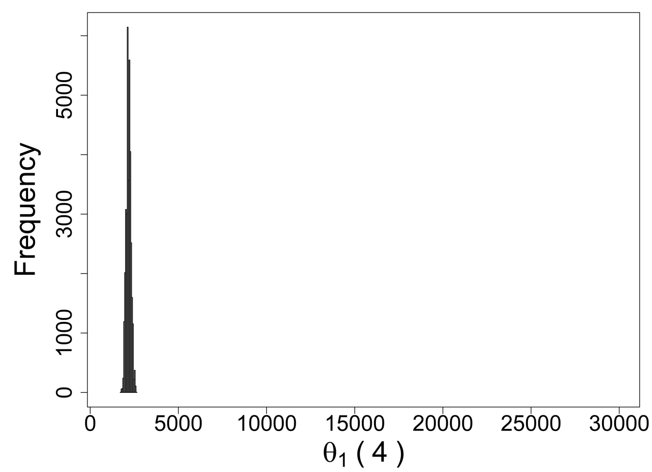

(d) Posterior distribution for $\theta_1(4)$

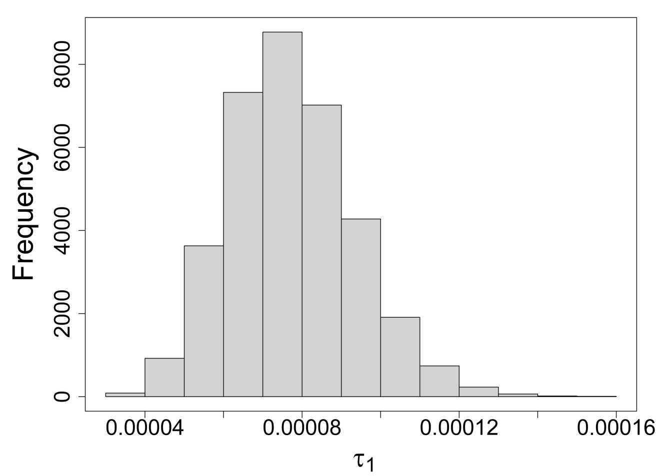

(e) Posterior distribution for τ_1

Fig. 6 Posterior distributions for Assembly 1

Simulated Field Test Data for Classification

For Bayesian classification, a set of simulated field data was generated from the high-fidelity Digital Twin simulation under the same true parameter settings used for the generation of simulated laboratory data. The high-fidelity Digital Twin was run using the same longitudinal velocity. However, instead of a speed bump road profile, stochastic road profiles with surface roughness $G_d = 1024 * 10^{-6} m^3/cycles$ conforming to class D road according to ISO 8608 [15] were used. An example of such road profile is shown in Figure 7.

500 such road profiles were generated, and high-fidelity Digital Twin simulations were run on each of those road profiles. The simulation time was 15 seconds, with the first 6 seconds under smooth road conditions and then rough road (Class D) from 6 to 15 seconds. The normal force time history between 10 and 15 seconds, sampled at 0.001 seconds, was taken. The Gaussian noise with the same mean and variance as for the laboratory data was sampled and added to the model outputs to obtain 500 sets of simulated field data.

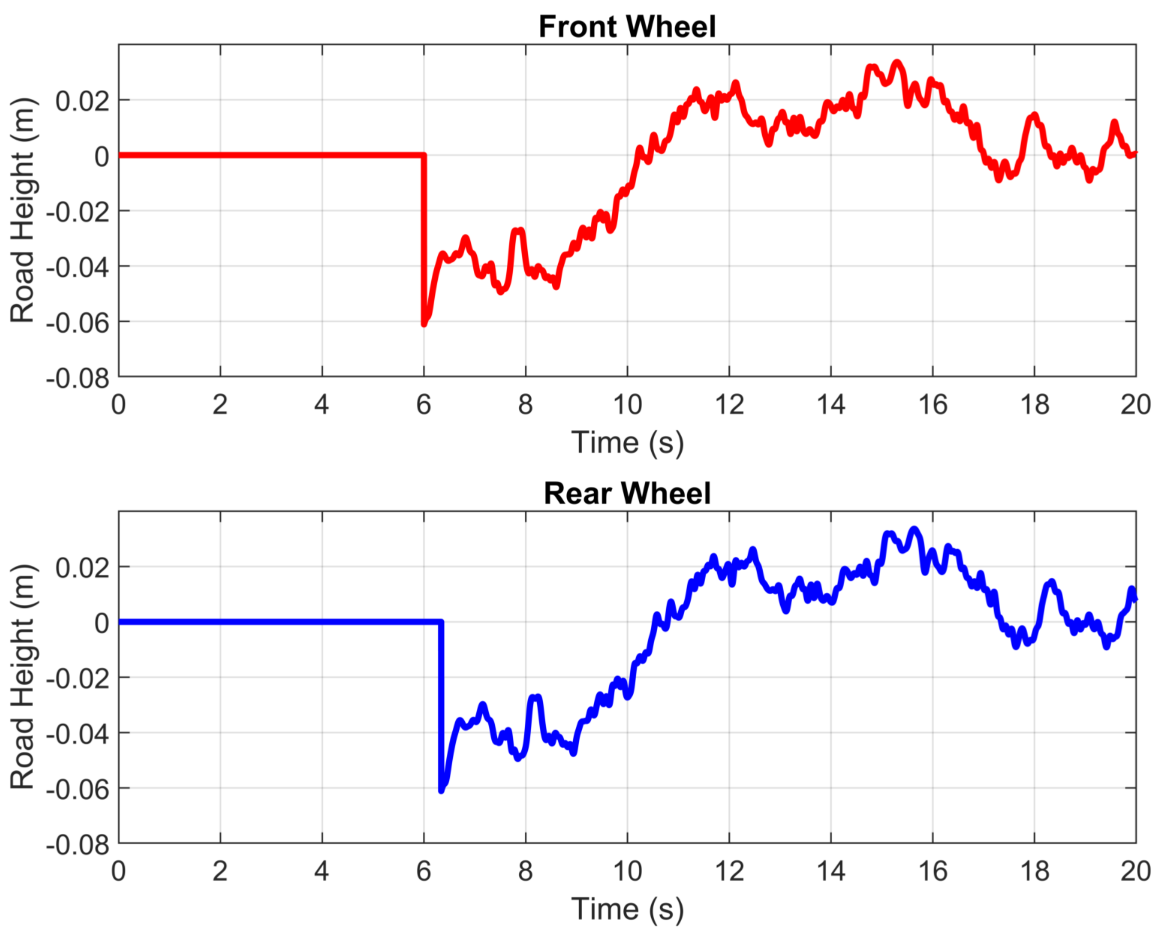

Fig. 7 Example of Stochastic Road Profile

Synthetic Field Data Generation

From the 35000 samples in the posterior distributions of each assembly, 10000 random samples were taken (10000 samples were found to be sufficient to represent the respective posterior distributions). A library of 50000 ISO 8608 class D road profiles was created. For each of the 10000 samples from the posterior distributions of each assembly, the Digital Twin simulation was run under 5 randomly selected stochastic road profiles, generating a total of 50000 model outputs from each assembly. The precision parameters for each assembly were sampled from their posterior distribution, and the error was sampled from a normal distribution with 0 mean and variance equal to the inverse of the precision sampled. The errors were

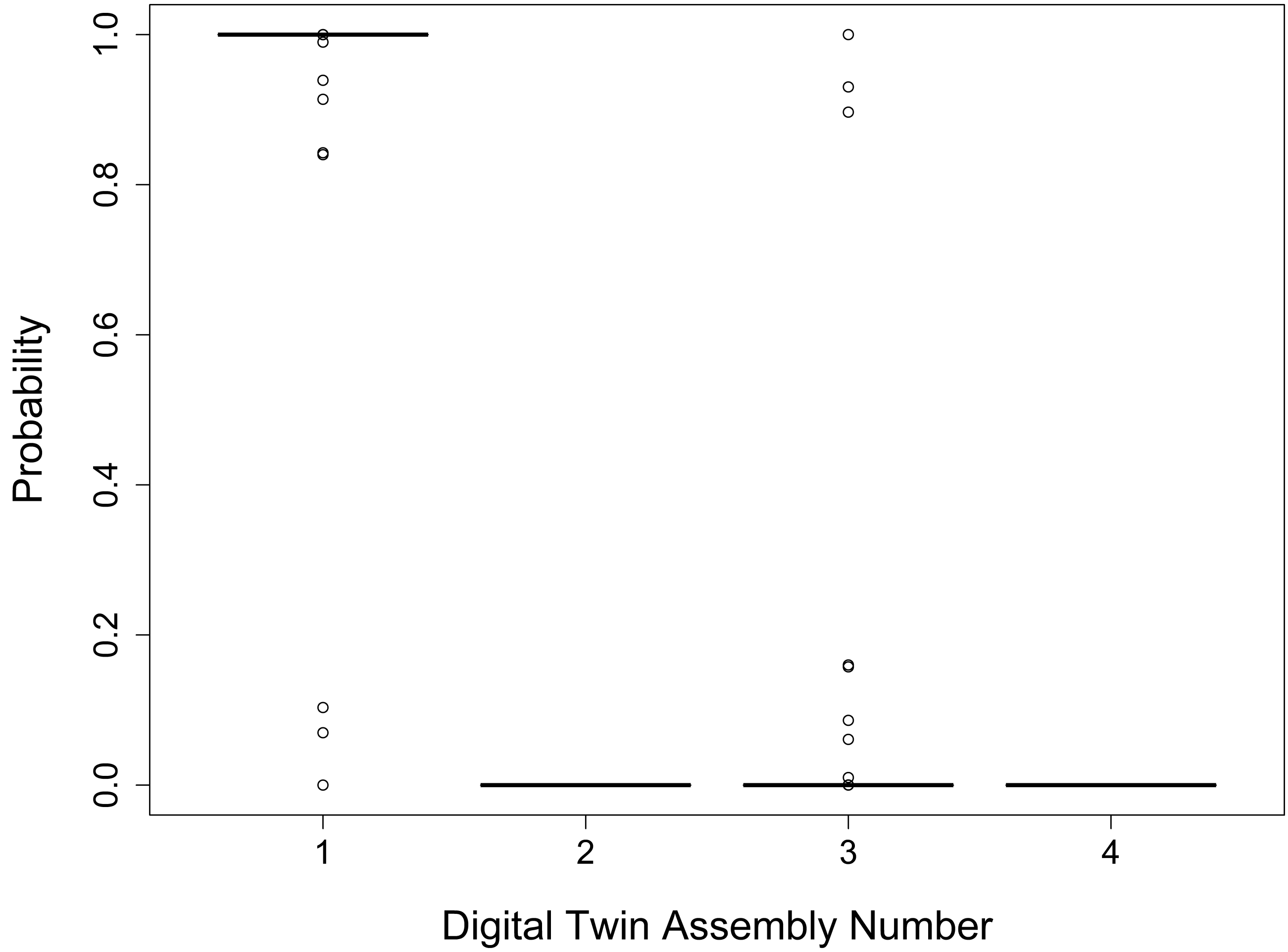

Fig. 8 Boxplot of the probability of selecting each assembly

added to each of those 50000 model outputs from the corresponding assembly to obtain the synthetic field data. The data were then fitted to a multivariate normal distribution. This yielded a unique mean and covariance corresponding to each of the assemblies.

Bayesian Classification

Finally, the probability of observing each of the 500 sets of simulated field data, given that the data came from each of the assemblies (in other words, the probability of observing the data given the mean and covariance structure of each assembly) were evaluated. It was observed that the probability of selecting the true assembly (assembly M_1) is highest for most of those 500 runs, as shown in the box and whisker plot 8 below. This shows that the Bayesian assembly tool can select the correct model with a very high probability.

Conclusion

A mixture-based Bayesian Assembly Tool is proposed that selects the set of Digital Twin subsystems with different levels of fidelities that best fit observed data. First, laboratory test data is acquired either from a laboratory test or from a simulation using a higher fidelity Digital Twin assembly. The Digital Twin assemblies with combinations of different fidelity level subsystem models are created and calibrated to the experimental data. The Griddy Gibbs calibration methodology based on the Bayesian framework is adopted. The result of calibration is posterior distributions of the uncertain parameters and the precision parameter associated with the model error. These posterior distributions are used to inform the Bayesian Assembly Tool on the probability distributions of the uncertain parameters of the Digital Twin assemblies. Finally, based on the likelihood of observing the field test data given those distributions, the best-fit model is selected. The application of the Bayesian Assembly Tool is validated using four sets of Digital Twin assemblies with a combination of two tire models, the Fiala model and the PAC2002 model, and two suspension models, MacPherson suspension and solid axle suspension. The Bayesian Assembly Tool was able to select the correct Digital Twin assembly with high accuracy.

Acknowledgments This work was supported by Clemson University's Virtual Prototyping of Autonomy Enabled Ground Systems (VIPR-GS) under Cooperative Agreement W56HZV-21-2-0001 with the US Army DEVCOM Ground Vehicle Systems Center (GVSC).

References

1. Sara Blasco Román and Till Böttjer. "A Methodological Approach to Prioritize Digital Twin Development in Manufac- turing". In: *Applied Stochastic Models in Business and Industry* 41.3 (2025), e2889. DOI: https://doi.org/10.1002/asmb.2889. eprint: https://onlinelibrary.wiley.com/doi/pdf/10.1002/asmb.2889. URL: https://onlinelibrary.wiley.com/doi/abs/10.1002/asmb.2889.
2. National Academy of Engineering, Engineering National Academies of Sciences, and Medicine. *Foundational Research Gaps and Future Directions for Digital Twins*. Washington, DC: The National Academies Press, 2024. ISBN: 978-0-309-70042-9. DOI: 10.17226/26894. URL: https://nap.nationalacademies.org/catalog/26894/foundational-research-gaps-and-future-directions-for-digital-twins.
3. Michael Grieves and John Vickers. "Digital Twin: Mitigating Unpredictable, Undesirable Emergent Behavior in Complex Systems". In: *Transdisciplinary Perspectives on Complex Systems: New Findings and Approaches*. Ed. by Franz-Josef Kahlen, Shannon Flumerfelt, and Anabela Alves. Cham: Springer International Publishing, 2017, pp. 85–113. ISBN: 978-3-319-38756-7. DOI: 10.1007/978-3-319-38756-7_4. URL: https://doi.org/10.1007/978-3-319-38756-7_4.
4. The MathWorks Inc. *Combined Slip Wheel 2DOF*. URL: https://www.mathworks.com/help/vdynblks/ref/combinedslipwheel2dof.html.
5. The MathWorks Inc. *Fiala Wheel 2DOF*. URL: https://www.mathworks.com/help/vdynblks/ref/fialawheel2dof.html.
6. Stephen Jay Wright et al. "An Efficient Statistical Inference Approach for Model Calibration Using Griddy Gibbs Sam- pling". In: *ASCE-ASME J Risk and Uncert in Engrg Sys Part B Mech Engrg* 11.3 (2025).
7. M.G. Kapteyn et al. "Data-driven physics-based digital twins via a library of component-based reduced-order models". In: *International Journal for Numerical Methods in Engineering* 123.13 (2022), pp. 2986–3003. DOI: https://doi.org/10.1002/nme.6423. eprint: https://onlinelibrary.wiley.com/doi/pdf/10.1002/nme.6423. URL: https://onlinelibrary.wiley.com/doi/abs/10.1002/nme.6423.
8. Michael G. Kapteyn, David J. Knezevic, and Karen Willcox. "Toward predictive digital twins via component-based reduced-order models and interpretable machine learning". In: *AIAA Scitech 2020 Forum*. DOI: 10.2514/6.2020- 0418. eprint: https://arc.aiaa.org/doi/pdf/10.2514/6.2020-0418. URL: https://arc.aiaa.org/doi/abs/10.2514/6.2020-0418.
9. Guesuk Lee et al. "Review of statistical model calibration and validation—from the perspective of uncertainty structures". In: *Structural and Multidisciplinary Optimization* 60 (Oct. 2019). DOI: 10.1007/s00158-019-02270-2.
10. MathWorks. *fmincon*. Accessed: 2025-03-22. n.d. URL: https://www.mathworks.com/help/optim/ug/fmincon.html.
11. MathWorks. *Independent Suspension - MacPherson*. Accessed: 2025-03-20. n.d. URL: https://www.mathworks.com/help/vdynblks/ref/independentsuspensionmacpherson.html.
12. MathWorks. *Solid Axle Suspension - Coil Spring*. n.d.
13. MathWorks. *What is a Digital Twin?* Accessed: 2025-03-20. n.d. URL: https://www.mathworks.com/discovery/digital-twin.html.
14. Johannes Mayer et al. "A decision-making methodology for selecting digital twin applications in the product service phase considering value and effort". In: *Production Engineering* (May 2025). DOI: 10.1007/s11740-025-01350-1.
15. Internationale Organisation für Normung. *ISO 8608 : Mechanical Vibration, Road Surface Profiles, Reporting of Measured Data: Inte* International Organization for Standardization, ISO, 1995. URL: https://books.google.com/books?id=1kyioAEACAAJ.
16. Hans B. Pacejka. *Tire and Vehicle Dynamics*. 3rd. Oxford: Elsevier, 2012. ISBN: 978-0123820301.
17. T.G. Ritto, S. Beregi, and D.A.W. Barton. "Reinforcement learning and approximate Bayesian com- putation for model selection and parameter calibration applied to a nonlinear dynamical system". In: *Mechanical Systems and Signal Processing* 181 (2022), p. 109485. ISSN: 0888-3270. DOI: https://doi.org/10.1016/j.ymssp.2022.109485. URL: https://www.sciencedirect.com/science/article/pii/S0888327022005970.
18. Simon Rouchier, Mickaël Rabouille, and Pierre Oberlé. "Calibration of simplified building energy models for param- eter estimation and forecasting: Stochastic versus deterministic modelling". In: *Building and Environment* 134 (2018), pp. 181–190. ISSN: 0360-1323. DOI: https://doi.org/10.1016/j.buildenv.2018.02.043. URL: https://www.sciencedirect.com/science/article/pii/S036013231830115X.
19. Concetta Semeraro et al. "Digital twin paradigm: A systematic literature review". In: *Computers in Industry* 130 (2021), p. 103469. ISSN: 0166-3615. DOI: https://doi.org/10.1016/j.compind.2021.103469. URL: https://www.sciencedirect.com/science/article/pii/S0166361521000762.
20. Angira Sharma et al. "Digital Twins: State of the art theory and practice, challenges, and open research questions". In: *Journal of Industrial Information Integration* 30 (2022), p. 100383. ISSN: 2452-414X. DOI: https://doi.org/10.1016/j.jii.2022.100383. URL: https://www.sciencedirect.com/science/article/pii/S2452414X22000516.
21. Sumit Singh et al. "Challenges of Digital Twin in High Value Manufacturing". In: Oct. 2018. DOI: 10.4271/2018-01- 1928.
22. Hannah Stewart. "Creation and Validation of a Novel Bayesian Calibration Method with Griddy Gibbs Sampling". All Theses. Paper 4177. Master's thesis. Clemson University, 2023. URL: https://open.clemson.edu/all_theses/4177.

23. Thomas Titscher et al. "Bayesian model calibration and damage detection for a digital twin of a bridge demonstrator". In: *Engineering Reports* 5.11 (2023), e12669. DOI: https://doi.org/10.1002/eng2.12669. eprint: https://onlinelibrary.wiley.com/doi/pdf/10.1002/eng2.12669. URL: https://onlinelibrary.wiley.com/doi/abs/10.1002/eng2.12669.
24. Rui Tuo and C. F. Jeff Wu. *A theoretical framework for calibration in computer models: parametrization, estimation and convergence* 2015. arXiv: 1508.07155 [stat.ME]. URL: https://arxiv.org/abs/1508.07155.
25. Seongjin Yun, Jun-Hong Park, and Won-Tae Kim. "Data-centric middleware based digital twin platform for dependable cyber-physical systems". In: *2017 Ninth International Conference on Ubiquitous and Future Networks (ICUFN)*. 2017, pp. 922–926. DOI: 10.1109/ICUFN.2017.7993933.
26. Lin Zhang, Longfei Zhou, and Berthold K.P. Horn. "Building a right digital twin with model engineering". In: *Journal of Manufacturing Systems* 59 (2021), pp. 151–164. ISSN: 0278-6125. DOI: https://doi.org/10.1016/j.jmsy.2021.02.009. URL: https://www.sciencedirect.com/science/article/pii/S0278612521000455.

Appendix

Table 3 Description of Variables Used in the Equation (3)

Variable	Description
q_{v2}	Tire stiffness variation coefficient with speed
Ω	Wheel rotational velocity
R_0	Unloaded radius
Vo	Measurement speed at test bench
q_{FCX}	Load response to longitudinal force
F_x	Longitudinal force
F_{z0}	Normal wheel load
q_{Fcy}	Load response to lateral force
F_y	Lateral force
q_{Fz1}	Tire vertical stiffness coefficient (linear)
q_{Fz3}	Camber dependency of the tire vertical stiffness
v	Camber (inclination) angle
ρ_z	Tire vertical deflection
q_{Fz2}	Tire vertical stiffness coefficient (quadratic)
p_{pFz1}	Factor to include effect of tire pressure
d_{pi}	Normalized inflation pressure
λ_{cz}	Scale factor for vertical tire stiffness
K_z	Tire vertical damping
qreo	Correction factor for measured unloaded radius
q_{Fcx1}	Tire stiffness interaction with F_x
q_{FCY1}	Tire stiffness interaction with camber

Table 4 Description of Variables Used in the Equation (4)

Variable	Description
$F_{wz_{a,t}}$	Suspension force applied to the wheel on axle a, wheel t along wheel-fixed z-axis.
$F_{z\text{O}_a}$	Vertical suspension spring preload force applied to the wheels on axle a.
k_{z_a}	Vertical spring constant applied to wheels on axle a.
$m_{\text{hsteer }a}$	Steering angle to vertical force slope applied at wheel carrier for wheels on axle a.
$\delta_{\text{steer }a,t}$	Steering angle input for axle a, wheel t.
C	Vertical damping constant applied to wheels on axle a.
$F_{\text{zhstop }a,t}$	Vertical hardstop force at axle a, wheel t, along the inertial-fixed z-axis.
$F_{zaswya,t}$	Vertical anti-sway force at axle a, wheel t, along the inertial-fixed z-axis.
$z_{v_{a,t}}, z^{\cdot}v_{a,t}$	Vehicle displacement and velocity at axle a, wheel t, along the inertial-fixed z-axis.
$z_{w_{a,t}}, z^{\cdot}w_{a,t}$	Wheel displacement and velocity at axle a, wheel t, along the inertial-fixed z-axis.

Table 5 Description of Variables Used in the Equation (5)

Variable	Description
$F_{wz_{a,t}}$	Suspension force applied to the wheel on axle a, wheel t along the wheel-fixed z-axis
$F_{wa_{z0}}$	Wheel and axle interface compliance constant
k_{wa_z}	Wheel and axle interface compliance constant
$z_{w_{a,t}}$	Wheel displacement at axle a, wheel t along the inertial-fixed z-axis
$z_{s_{a,t}}$	Suspension displacement at axle a, wheel t along the inertial-fixed z-axis
$\boldsymbol{C_{wa_z}}$	Wheel and axle interface damping constant
$z'w_{a,t}$	Wheel velocity at axle a, wheel t along the inertial-fixed z-axis
$z^*{}_{s_{a,t}}$	Suspension velocity at axle a, wheel t along the inertial-fixed z-axis

Table 6 Non-default parameter values of Fiala Tire model

Parameter	Label	Unit	Value
Brake type	-	-	Disc
Rolling Resistance	-	-	Magic Formula
Vertical Motion	-	-	Mapped stiffness and damping
Kinematic friction	muMin	-	.5
Static friction	muMax	-	.8
Wheel mass	MASS	kg	29.46
Maximum pressure	PRESMAX	Pa	1000000
Minimum pressure	PRESMIN	Pa	10000
Max allowable slip ratio (absolute	KPUMAX	-	1.5
Minimum allowable slip ratio (absolute)	KPUMIN	-	-1.5
Max allowable slip angle (absolute)	ALPMAX	rad	1.5
Minimum allowable slip angle (absolute)	ALPMIN	rad	-1.5
Maximum allowable camber angle	CAMMAX	rad	0.2
Minimum allowable camber angle	CAMMIN	rad	-0.2

Table 7 Non-default parameter values of Pac2002 Tire model

Parameter	Label	Unit	Value
Brake type	-	-	Disc
Maximum pressure	PRESMAX	Pa	1000000
Minimum pressure	PRESMIN	Pa	10000
Max allowable slip angle (absolute)	ALPMAX	rad	1.5
Minimum allowable slip angle (absolute)	ALPMIN	rad	-1.5
Maximum allowable camber angle	CAMMAX	rad	0.2
Minimum allowable camber angle	CAMMIN	rad	-0.2
Nominal pressure	NOMPRES	Pa	220000
Nominal normal force	FNOMIN	N	4000
Wheel mass	MASS	kg	29.46
Longitudinal stiffness	LONGITUDINAL_STIFFNESS	N/m	$1e7$
Lateral stiffness	LATERAL_STIFFNESS	N/m	$4.5e4$

Table 8 Non-default parameter values of MacPherson Suspension Model

Parameter	Label	Unit	Value
Toe angle at steering center	Toe	rad	0
Roll steer angle vs suspension height slope	RollStrgSlp	rad/m	0
Toe angle vs steering angle slope	ToeStrgSlp	-	0
Caster angle at steering center	Caster	rad	0
Caster angle vs suspension height slope	CasterHslp	rad/m	0
Caster angle vs steering angle slope	CasterStrgSlp	-	0
Camber angle at steering center	Camber	rad	0
Camber angle vs suspension height slope	CamberHslp	rad/m	0
Camber angle vs steering angle slope	CamberStrgSlp	-	0

Table 9 Non-default parameter values of Solid Axle Suspension model

Parameter	Label	Unit	Value
Axle and wheels lumped principal moment of inertia about longitudinal axis	AxlIxx	$kg * m^2$	62.37
Axle and wheels lumped mass	AxlM	kg	29.46
Wheel and axle interface compliance constant	KzWhlAxl	N/m	138031.61
Wheel and axle interface compliance preload	F0zWhlAxl	N	2907
Wheel and axle interface damping constant	CzWhlAxl	Ns/m	11490.97
Suspension spring preload	F0z	N	2907
Suspension maximum height	Hmax	m	0.25
Toe angle at steering center	Toe	rad	0
Roll steer angle vs suspension height slope	RollStrgSlp	rad/m	0
Toe angle vs steering angle slope	ToeStrgSlp	-	0
Caster angle at steering center	Caster	rad	0
Caster angle vs suspension height slope	CasterHslp	rad/m	0
Caster angle vs steering angle slope	CasterStrgSlp	-	0